Available online at www.sciencedirect.com
ScienceDirect
ELSEVIER
Ocean Engineering 35 (2008) 28–40
OCEAN ENGINEERING
www.elsevier.com/locate/oceaneng

Sailboat propeller drag

P.M. MacKenzie*, M.A. Forrester

Department of Mechanical Engineering, University of Strathclyde, Glasgow G1 1XJ, Scotland, UK

Received 15 March 2007; accepted 1 July 2007
Available online 10 July 2007

Abstract

All but the smallest classes of modern keelboats are fitted with inboard engines and consequently, when making way under sail, the craft experience parasitic drag due to trailing propellers and associated appendages. The variety of screw configurations used on sailing boats includes fixed-blade, feathering, and folding set-ups, with blades numbering two or three. Although the magnitude of the resultant drag is thought to have a significant influence on sailing performance, the published literature having regard to this problem is sparse. Here, the aim was to evaluate the drag effect of fixed-blade propellers of types commonly used on sailing craft. The results of towing tank tests on full-scale propellers are presented for the locked shaft condition; these are presented along with reconfigured data from the few previously published sources. For the case in which the propeller is allowed to rotate, tests were conducted on a typical screw with a range of braking torques being applied. It was hypothesised that the performance coefficients of the Wageningen B-Screw Series could be used to characterise adequately the types of screw of interest and that these could be extrapolated to enable prediction of the drag of a freewheeling propeller; an assessment of this formed part of the investigation.

Keywords: Drag; Experiment; Propeller; Sailboat; Towing tank

1. Introduction

For several decades, virtually all sailing yachts over about 8 m overall length (LOA) have been equipped with inboard engines driving through either fixed propeller shafts or, increasingly so, the more compact "saildrive" units. Some examples of common configurations are depicted in Fig. 1. Even race-oriented designs are, in general, equipped with quite substantial auxiliary power units, despite the penalty in sailing performance caused by the additional weight of the machinery and fuel, and the hydrodynamic drag arising from the extraneous appendages such as propellers and shafts.

An obvious way to achieve a reduction in hydrodynamic losses is to fit a propeller with folding or feathering blades. Nevertheless, a cursory survey of any winter lay-up yard will confirm that the majority of yachts used exclusively for cruising, and indeed a small proportion of those used for racing, are fitted with conventional fixed geometry two- or three-bladed propellers. There are several reasons for this. First of all, low-drag deployable propellers are mechanically complex and consequently have a high initial price — up to 10 times that of the fixed-blade equivalent. Having moving parts, and operating in an exposed and corrosive environment, they are prone to wear and damage. Some designs of folding propellers in particular, in which the blades are deployed by centrifugal force when the prop-shaft spins, have blade geometries which are compromised by the impositions of the deployment function such that their hydrodynamic efficiencies are relatively poor driving ahead, and are significantly worse for astern propulsion and manoeuvring, when compared to the fixed-blade alternatives. Finally, there appears to be no consensus in the sailing community, nor in racing handicap administration, nor in the sailboat design field, as to the actual gains to be had in sailing performance, in an objective and quantifiable sense, when the low drag configuration is employed in preference to fixed-blade propellers (some measure of the range of views may be gleaned from, for

*Corresponding author. Tel.: +44 141 548 2045; fax: +44 141 552 5105.
E-mail address: peter.mackenzie@strath.ac.uk (P.M. MacKenzie).

0029-8018/$ - see front matter © 2007 Elsevier Ltd. All rights reserved.
doi:10.1016/j.oceaneng.2007.07.004

Fig. 1. A variety of propulsion configurations commonly found on sailing boats. Clockwise from top left: fixed three-blade in aperture behind long keel; fixed three-blade on exposed shaft well behind fin keel; feathering three-blade on shaft, fin keel; folding two-blade, deployed; folding two-blade, folded; folding three-blade, folded, on sail-drive strut behind high aspect-ratio keel.

example: Henderson 1983; Johnson 1997; Skene 1938; and Warren 1972). Adding to this confusion is the myth of common currency among many yachtsmen that the practice of locking a fixed-blade propeller to prevent rotation results in less drag than would allowing it to freewheel. The present work seeks to address some of the more important aspects of these lacunae.

2. Existing hypotheses

Whilst, with obvious justification, the subject of ship propeller performance and efficiency has had a great deal of research effort devoted to it, the topic of parasitic propeller drag appears rarely in the literature.

Larsson and Eliasson (1994) proposed that the following relationship be used to estimate propeller resistance, R_P, in a boat design context:

$$R_P = 0.5\,\rho V^2\, C_{\mathrm{D}}\, A_P \tag{1}$$

and that the drag coefficients are:

$C_{\mathrm{D}} = 1.2$ for fixed blades, shaft locked.
$C_{\mathrm{D}} = 0.3$ for fixed blades, shaft free to rotate, zero braking torque.
$C_{\mathrm{D}} = 0.06$ for a two-blade folding propeller.

A_P is the projected frontal area of the propeller, V is the boat speed and ρ is the density of water. (They do not directly identify the source of these C_{D} values, and one assumes that the coefficient given for the locked shaft condition may simply be that of a flat disc, bluff body.) Part of the present work would be directed at assessing the veracity of this convenient approach.

Lurie and Taylor (1995) reported the results of their tests of a comprehensive range of sailboat propellers covering virtually all popular configurations. Their study was principally directed towards assessing the performance of each screw as a propulsion device but they also produced some measurements of the drag characteristics for the locked shaft condition (with regard to parasitic drag, this being the least desirable of all). In the concluding part of their work, they went on to allude to the possibility of being able to extrapolate propeller performance curves to predict the parasitic drag force for a notional speed of screw rotation, but stopped short of assessing the validity of this. One of the aims of our investigation was to develop this proposal further.

3. Proposed approaches

The main thrust of this work, therefore, was to establish the veracity of the existing hypotheses summarised above, and where appropriate, to assess possible refinements or alternatives. The investigation can thus be divided conveniently into two elements: consideration of the drag produced by freewheeling propellers and evaluation of the drag characteristics of propellers with locked shafts.

4. Investigation — freewheeling condition

4.1. Performance characteristics of propellers

The proposal being investigated in this part of the work is built around the following three forward-performance characteristics of propellers:

(i) *Advance ratio*:

$$J = \frac{V_A}{D \cdot n}, \tag{2}$$

where V_A is the velocity of advance of the propeller, D is the propeller diameter, and n is the rotational speed.

(ii) *Torque coefficient*:

$$K_Q = \frac{Q}{\rho D^5 n^2} \tag{3}$$

where Q is the torque on the propeller shaft.

(iii) *Thrust coefficient*:

$$K_T = \frac{T}{\rho D^4 n^2}, \tag{4}$$

where T is the thrust on the propeller.

In ship design practice, the relationship between these three parameters is used routinely to characterise individual designs of propeller (as propulsion devices) and this is usually depicted in the form shown schematically in Fig. 2. The curve for efficiency of propulsion, η, is also generally presented as shown along with these data but for our purpose, namely the prediction of propeller drag under sail, it is of less significance. For completeness, however, it may be noted that η is derived from the aforementioned parameters according to:

Propeller efficiency:

$$\eta = \frac{J \cdot K_T}{2\pi K_Q}. \tag{5}$$

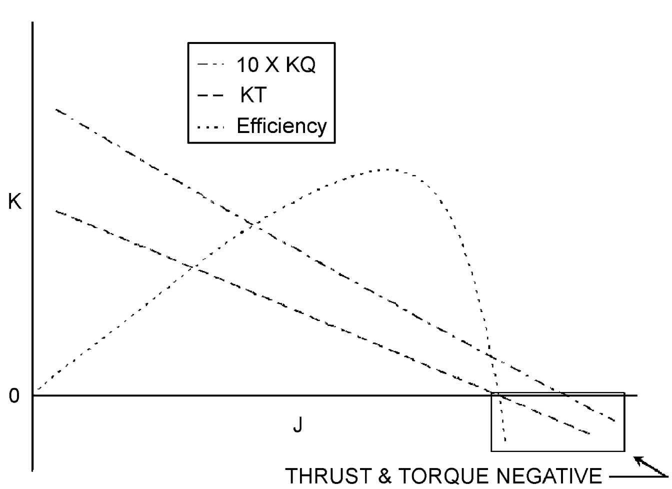

Fig. 2. Schematic depiction of propeller performance curves.

4.2. Frictional torque

A key part of our proposition is that, in cases where a vessel is making way under sail and its propeller is allowed to freewheel, the rotational frictional force on the propeller shaft, the negative torque, may be assumed to be constant for a given installation, regardless of, within realistic practical limits, the shaft speed of rotation. In practice, of course, factors such as stern gland tightness, gearbox oil viscosity (largely a function of temperature), bearing efficiency and wear, and so on, will influence the level of friction. Nevertheless, for virtually any boat among the types described in the introduction, the torque required to rotate the shaft should be readily measurable *in situ* using the most basic of apparatus; and obviously, account may be taken of the spectrum of frictional conditions for a given set-up if so required. The main point here is that, given a particular set of shaft friction conditions, then for all rotational speeds likely to be encountered in practice, the frictional torque, Q, can be assumed to be constant throughout the speed range. In this respect, we diverge from Lurie and Taylor who suggested that an estimated average speed of rotation, n, be used in the analysis. (Their thinking was that by fixing n, one would be able to obtain J for any value of velocity, and thus the relevant values of K_T could be extracted from the extrapolated performance chart. Hence, it would be a simple step to calculate the resultant negative thrust using Eq. (4), and thereby generate a chart of drag vs. velocity. Attractive though this would be, it is erroneous, as we will show, since a very wide band of rotational speed is observed in practice.)

4.3. Velocity of advance

For the purpose of this investigation, it is assumed that the velocity of advance, V_A, of the propeller is identical to, or can be related to, boat speed, V. In other words, the water flow experienced by the propeller is equal to the open-water flow past the hull, remote from the local influence of wake produced by the hull and its appendages, or that a suitable wake correction may be applied. Taylor's wake fraction is given by:

$$w = \frac{V - V_A}{V}$$

and hence

$$V_A = V(1 - w). \tag{6}$$

In the first instance, therefore, we will assume that $w = 0$; in practice, this may not be absolutely so, but for modern fin-keeled sailing boats, fitted with efficient, high aspect-ratio, airfoil section keels, the propeller is generally located well aft of the keel and below, rather than behind, the hull; thus the effect of wake interaction is to reduce V_A to not less than about 0.9 V (Larsson and Eliasson, 1994). On the other hand, if the propeller is behind an unfaired skeg, or in the case of older style long-keeled yachts, dual-purpose motor sailers, and on some large modern sailing vessels, where the propeller is usually mounted behind the hull or in an aperture behind, and close to, the dead-wood of the keel, w may be much higher (Skene, 1938, predicts a value of 0.2 in some such cases). For sailing vessels, the range of values of w, from virtually zero to about 0.2, is therefore very much narrower than that encountered in power driven vessels (e.g., Gerr, 1989); nevertheless, for any situation, appropriate adjustment to account for conditions of reduced flow can readily be made in those cases in which it is of significance. (Some contrasting keel types are depicted, *inter alia* in Fig. 1.)

4.4. Relating velocity of advance to propeller drag

The key assumption in the proposed approach is that the braking torque imparted on the propeller shaft is constant throughout the speed range. It follows then from Eq. (3) that, for such an installation where Q is constant, for every value of K_Q, there is a unique value of shaft speed, n; similarly, there is a single corresponding value of J. In such a propulsion system set-up, the variables in Eqs. (2)–(4) are V_A, n and T. Since the remaining factors are constant (namely, the frictional torque and the screw diameter) and can be measured quite straightforwardly, we can draw (2) and (3) together to give

$$V_A = JD\sqrt{\frac{Q}{\rho D^5 K_Q}}. \tag{7}$$

Here, the proposal is to apply data read from the usual curves of K_Q and K_T vs. J, as illustrated in Fig. 2, but extrapolated into the regime where thrust and torque are negative, as indicated in the same figure. By taking Eq. (6) in conjunction with the appropriate performance chart (viz., Fig. 2) for a given propeller pattern, we can see that velocity of advance, V_A, can be determined for any given combination of J and K_Q, assuming that we have constant shaft torque, Q. Now, by extrapolating the curve for K_T into the negative zone also, one is able to obtain a value of K_T, and consequently thrust, T, for those very combinations of J and K_Q. In summary, the variables required to enable convenient generation of a curve of (negative) thrust vs. velocity are present as the key dimensions of the screw together with the braking torque on the shaft; these are conveniently measurable in a practical sense. An important feature of this approach is that if we are in possession of a relationship which accurately models K_T and K_Q vis-à-vis J, then we have no need to measure n in order to be able to predict drag. The item absent thus far in the study is a performance chart appropriate to the particular screw pattern of interest.

4.5. Wageningen B-Screw Series

The well-known series of open-water systematic tests of over 120 model screws conducted at the Netherlands Ship Model Basin produced a wealth of data aimed principally at applications in preliminary ship design studies. As well as covering a wide range of operating conditions, the tests encompassed the effects of blade number, pitch ratio, expanded area ratio, blade outline and blade thickness (van Lammeren et al., 1969). By multiple regression analysis, these data have been reduced to polynomials, and hence predictive performance curves can thus be predicted for a very broad range of permutations of screw configuration (Oosterveld and van Oossanen, 1975; van Manen and van Oossanen, 1988). In brief, the performance predictions can be condensed to:

$$K_T = f_1(J, P/D, A_E/A_0, Z, Re),$$

$$K_Q = f_2(J, P/D, A_E/A_0, Z, Re),$$

where P is the propeller pitch; D is the diameter; A_E is the expanded area, the developed area of the screw outside the hub; $A_0 = \pi D^2/4$ is the disc area, Z is the number of blades and Re is Reynolds number.

Whilst the Wageningen work was directed towards large commercial and naval vessels, the models tested were, in the main, of $D = 0.24$ m and therefore similar in size to or, indeed, slightly smaller than, propellers fitted to most auxiliary yachts. (A significant observation, therefore, is that the Wageningen tests were conducted at Reynolds numbers of identical order of magnitude to those experienced by full-scale sailboat propellers, thus engendering some confidence that, in this respect at least, the B-Screw comparisons are appropriate.) The B-Screw Series studies include very precise specifications for all of the propeller dimensions. However, the results have since been widely used to predict approximately the performance of propellers whose geometry may diverge somewhat from the specified standard (a practice described, for example, by Benini, 2003). One is therefore drawn to speculate, *prima facie*, that the extent to which the B-Screw Series results may be used to characterise yacht screws may be worthy of investigation. Consequently, one of the objectives here was to assess whether the predicted forward performance curves for a sailboat screw could be adapted to provide us with a sufficiently accurate prediction of propeller drag. As the first step towards this, the predicted characteristics generated using B-Series polynomials were compared with some of the experimental data for forward performance of sailboat screws previously published by Lurie and Taylor.

4.6. Method of predicting forward performance curves

The coefficients and terms of the K_T and K_Q polynomials of the Wageningen B-Series (*op cit*) are presented in Tables 1 and 2, but re-organised for the present work into a form more convenient for programming.

Thus, for any combination of P/D, A_E/A_0, and Z, it is a relatively straightforward matter to develop a computer program to predict the values of K_T and K_Q for the range

Table 1

$C_{t,u,v}$	t	u	v	$K_T = a + bJ + cJ^2 + dJ^3$
0.008804960	0	0	0	$a = \sum_{t,u,v} C_{t,u,v} \cdot (P/D)^t \cdot (A_E/A_0)^u \cdot Z^v$
0.166351000	1	0	0	
0.158114000	2	0	0	
0.415437000	2	1	0	
0.014404300	0	0	1	
0.014348100	1	0	1	
−0.012589400	0	1	1	
−0.133698000	3	0	0	
0.006384070	6	0	0	
−0.050721400	0	2	0	
−0.008417280	3	0	1	
−0.031779100	3	1	1	
−0.004107980	2	2	1	
−0.000606848	0	0	2	
0.000690904	0	1	2	
0.004217490	3	1	2	
−0.001465640	3	2	2	
−0.204554000	0	0	0	$b = \sum_{t,u,v} C_{t,u,v} \cdot (P/D)^t \cdot (A_E/A_0)^u \cdot Z^v$
−0.481497000	1	1	0	
0.060682600	1	0	1	
0.010968900	0	1	1	
0.010465000	6	2	0	
0.016842400	3	0	1	
0.018604000	0	2	1	
−0.004981900	0	0	2	
−0.001636520	2	0	2	
−0.000328787	6	0	2	
−0.147581000	0	1	0	$c = \sum_{t,u,v} C_{t,u,v} \cdot (P/D)^t \cdot (A_E/A_0)^u \cdot Z^v$
−0.053005400	0	0	1	
−0.001327180	6	0	0	
0.085455900	0	2	0	
−0.006482720	6	2	0	
0.002598300	0	0	2	
0.000116502	6	0	2	
0.168496000	0	1	0	$d = \sum_{t,u,v} C_{t,u,v} \cdot (P/D)^t \cdot (A_E/A_0)^u \cdot Z^v$
−0.050447500	0	2	0	
−0.001022960	3	0	1	
−0.000560528	0	0	2	
0.000056523	6	1	2	

Table 2

$C_{t,u,v}$	t	u	V	$K_Q = e + fJ + gJ^2 + hJ^3$
0.003793690	0	0	0	$e = \sum_{t,u,v} C_{t,u,v} \cdot (P/D)^t \cdot (A_E/A_0)^u \cdot Z^v$
0.003447780	2	0	0	
−0.040881100	1	1	0	
0.188561000	2	1	0	
0.005136960	1	0	1	
−0.026940300	2	1	1	
0.016188600	3	1	0	
0.015896000	0	2	0	
−0.050278200	1	2	0	
−0.039772200	3	2	0	
−0.003500240	6	2	0	
−0.000313912	6	0	1	
−0.001421210	6	1	1	
0.012680300	2	2	1	
0.003342680	6	2	1	
0.001553340	2	1	2	
0.000302683	6	1	2	
−0.000184300	0	2	2	
−0.000425399	3	2	2	
−0.000465900	6	2	2	
−0.032241000	1	0	0	$f = \sum_{t,u,v} C_{t,u,v} \cdot (P/D)^t \cdot (A_E/A_0)^u \cdot Z^v$
−0.108009000	1	1	0	
−0.003708710	0	0	1	
0.020944900	1	0	1	
0.004383880	1	1	1	
0.003180860	3	1	0	
0.047172900	0	2	0	
−0.003836370	0	2	1	
−0.001834910	1	0	2	
0.000269551	0	1	2	
0.000055419	6	2	2	
0.008865230	0	0	0	$g = \sum_{t,u,v} C_{t,u,v} \cdot (P/D)^t \cdot (A_E/A_0)^u \cdot Z^v$
−0.088538100	1	1	0	
0.004743190	1	0	1	
−0.007234080	0	1	1	
0.041712200	2	2	0	
−0.003182780	3	2	1	
0.000832650	0	1	2	
0.055808200	0	1	0	$h = \sum_{t,u,v} C_{t,u,v} \cdot (P/D)^t \cdot (A_E/A_0)^u \cdot Z^v$
0.019628300	0	2	0	
−0.030055000	1	2	0	
−0.010685400	0	0	1	
0.001109030	3	0	1	
0.003598500	0	1	1	
0.000112451	2	0	2	
−0.000029723	6	0	2	
0.000086924	3	2	2	

of values of J in which we are interested, viz:

$$K_T = a + bJ + cJ^2 + dJ^3 \tag{8}$$

and

$$K_Q = e + fJ + gJ^2 + hJ^3. \tag{9}$$

4.7. Comparison with experiment — forward performance

The experimental work conducted by Lurie and Taylor (1995) in a variable pressure water tunnel at the Marine Hydrodynamics Laboratory of Massachusetts Institute of Technology, was aimed at comparing several practical aspects of full-scale sailboat propellers: forward performance; crash-back; and locked drag. Included in their published results are forward performance curves covering the wide range of propeller configurations found on sailboats: fixed, folding, feathering, two-bladed and three-bladed.

None of the screws replicated the exact geometry of a standard Wageningen B-Series screw, but of interest here in the first instance is the extent to which we may be able to relate the available polynomials for K_T and K_Q to the actual measured performance of some typical fixed-blade yacht propellers. Thus, Figs. 3a and b depict curves derived for the present study using the 'Wageningen' polynomials, employing the key geometric features (diameter, pitch, EAR) of two fixed-blade propellers tested in the MIT work. Alongside our predicted values, we have imposed curves of measured performance which we have computed using data extracted from the drag vs. velocity results previously published (*ibid*).

There is good agreement between predicted B-Screw characteristics and those derived from the available experimental data. Indeed, in Fig. 3a the similarities between the two sets of data are remarkable. Both screws were produced by the same manufacturer, are very widely used, and were of patterns which, apart from the blade section details, part-airfoil and part-ogival, were qualitatively quite similar in geometry to their respective B-Screw equivalents. Sailboat fixed-blade propellers generally have similar blade cross-sections to the two cited (Gerr, 1989) and based on this limited assessment, and with a little caution, one may adopt the predictions of B-Screw characteristics to this extent. In the absence of further study, however, one should be guarded in using the B-Screw results for other types of blade whose geometries may nullify this approach; it should be noted that some types of sailboat propeller, notably all folding propellers, but others besides, have geometries which depart markedly from the B-Screw standard.

Of particular interest in the present work is the observation that, especially in those areas in Figs. 3a and b corresponding to minimum thrust (i.e., high values of J), the experimental curves of K_T and K_Q are predicted quite accurately by the respective polynomials. It appears, therefore, that the performance of fixed-blade sailboat screws of typical non-radical geometries might, indeed, be modelled, adequately, for forward propulsion and this provided justification for proceeding with the next stage of the investigation.

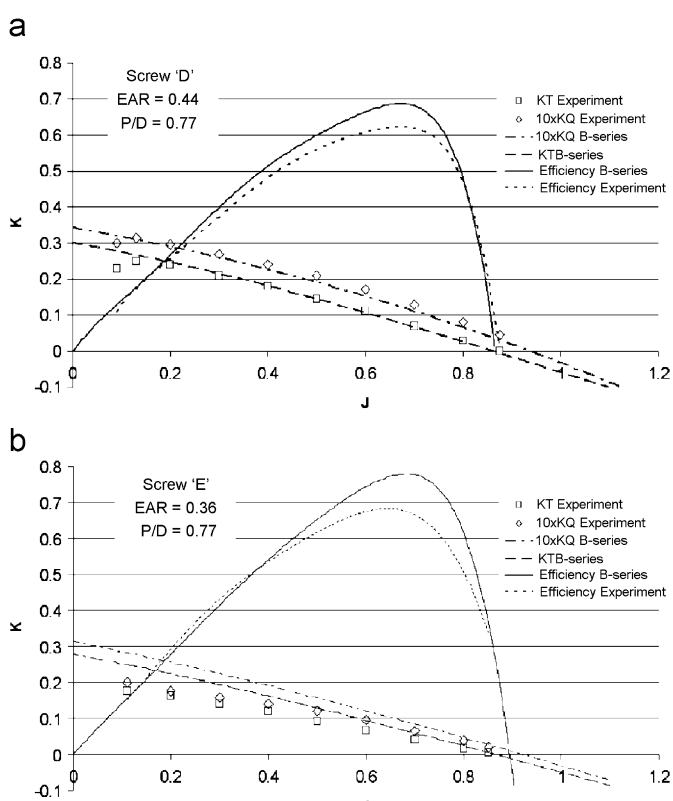

Fig. 3. (a) Comparison of B-Screw predicted performance curves, for three-blade screw, with water tunnel results of Lurie and Taylor (1995) for screw 'D'. Key dimensions are given in Table 3. (b) Comparison of B-screw predicted performance curves, for two-blade screw, with water tunnel results of Lurie and Taylor (1995) for screw 'E'. Key dimensions are given in Table 3.

4.8. *Experimental evaluation of drag as a function of torque (brake) loadings*

The information we wish to access is contained in the tail end of the K_T, K_Q vs. J curves, as highlighted in Fig. 2. The experimental work which was carried out to assess this relationship between braking torque and hydrodynamic drag was set up in such a way as to give a reasonable approximation of the conditions pertaining to a modern fin-keeled yacht. The short shaft on which the propeller was mounted was supported in roller bearings enclosed within a strut which was of similar dimensions to the 'P-bracket' which, on fin-keeled yachts, typically supports the end- bearing of the external propeller shaft immediately ahead of the propeller itself. The bearing housing was designed to contain a shaft-speed transducer also, together with an adjustable friction brake on the shaft. Close to its mounting on the tow-tank carriage, the strut incorporated an electronic load cell for drag measurement. A schematic of the layout is depicted in Fig. 4. The test runs were conducted with the propeller trailing behind the support strut and bearing, and with the screw hub immersed to a depth of 1 m.

The tests were conducted in a 70 m towing tank at the Marine Hydrodynamics Laboratory of the Universities of Glasgow and Strathclyde. This is 4.6 m wide with a depth

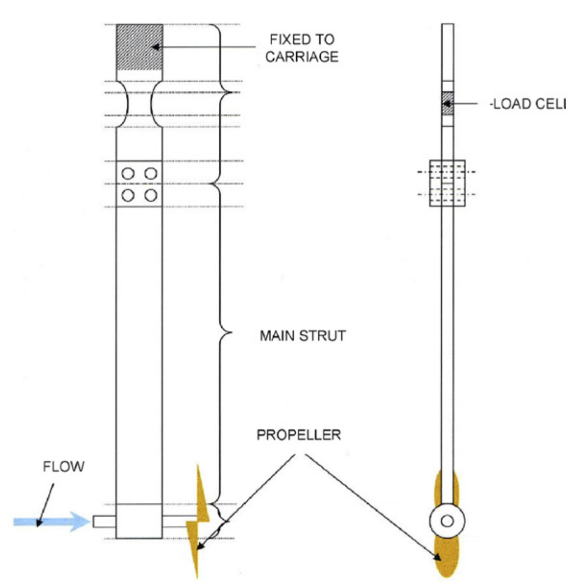

Fig. 4. Schematic of strut for towing tank tests.

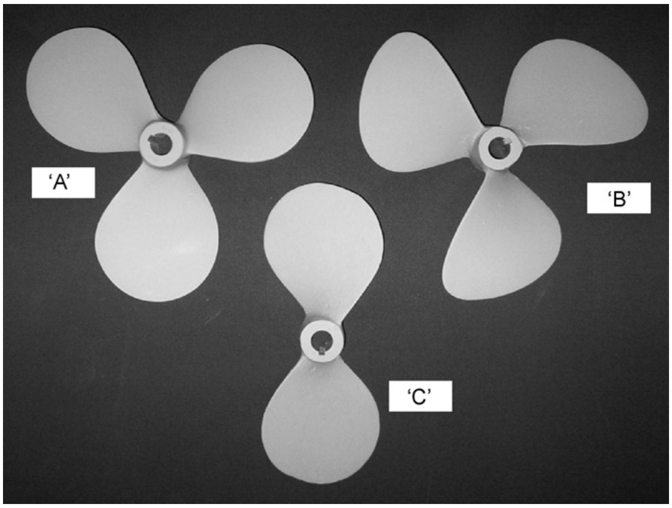

Fig. 5. Propellers tested in towing tank. Key dimensions are given in Table 3.

of 2.5 m, and containing fresh water which was at a temperature of 13 °C during the present work.

The propeller used in this section of work (propeller 'A' in Fig. 5) was of a simple general purpose pattern commonly found on yachts, with blade shape of round so-called 'turbine' pattern, no skew and 6° of rake. The pitch and diameter were 0.152 and 0.305 m, respectively (6 and 12 in). The expanded area ratio, A_E/A_0, (also EAR) was 54% and the hub area, at 18% of the total disc area, was slightly less than the B-Series norm of 20%; the chord length, $C_{0.75}$, at 0.75 of radius, R, from the hub centre, was 0.11 m. In keeping with modern practice in small-craft screw design (Gerr, 1989) the blades were of combined airfoil/ogival geometry, having airfoil section worked in from the roots to $0.7R$ and ogival over the remainder (i.e., flat on the thrust face, rounded on the suction surface); in this respect in particular, there is some departure from the B-Series geometry. The screw was manufactured in manganese bronze.

Tests were conducted over a range of braking torque settings from the minimum setting of the rig, 0.21 N m, up to fully locked. (It is worth noting here that Warren (1972) estimated that the practical range of frictional torque for vessels of the size outlined above was about 0.8–3 Nm; to some extent, this can be confirmed by a survey undertaken by the authors, but with the lower end of the range being extended to about 0.2 Nm.) Carriage speeds between 0.52 and 3.09 m/s (1–6 knots) were used and the resultant propeller shaft speeds, n, observed during the programme were within the range 2–15 revolutions per second (120–900 rpm), depending, of course, upon the velocity, V_A, and magnitude of the preset braking torque, Q.

4.9. Reynolds number effects

The coefficients in Tables 1 and 2 are for a Reynolds number of 2×10^6. The Reynolds numbers in the present work, $Re_{0.75}$, may be evaluated for the chord length at $0.75R$, the conditions at which point have been shown to be representative of the whole blade (Oosterveld and van Oossanen, 1975). $Re_{0.75}$ is obtained from:

$$Re_{0.75} = \frac{C_{0.75}\sqrt{V_A^2 + (0.75\pi nD)^2}}{\nu}, \tag{10}$$

where ν is the kinematic viscosity, $1.21\times10^{-6}\,\mathrm{m^2/s}$ for the present work. Using this approach, a representative range of values for $Re_{0.75}$ for the operating conditions of the tests performed in the Glasgow and Strathclyde tank was found to be approximately 5×10–9×10^5. In a manner similar to that employed in the main portion of their work, Oosterveld and van Oossanen applied multiple regression analysis to a relatively limited number of screw tests to obtain polynomials aimed at enabling corrections to be made to predicted K_T and K_Q values for conditions of $Re_{0.75}$ between 2×10^6 and 10^8, covering the range which was of practical interest to them, namely the conditions experienced in large commercial and naval vessels. Thus:

$$\Delta K_T = f_3(J, P/D, A_E/A_0, Z, (\log Re\,0.75 - 0.301)),$$

$$\Delta K_Q = f_4(J, P/D, A_E/A_0, Z, (\log Re\,0.75 - 0.301)).$$

In the work presented here, the largest correction would be associated with the lowest value of Reynolds number encountered which was $Re = 5\times10^5$. The influence of this was calculated by extrapolation of the Wageningen corrections and was found to be insignificant for the present purpose; for example, $\Delta K_T = 0.3\%$ of the uncompensated value of K_T, whilst ΔK_Q was predicted to be not more than 4% of the unadjusted K_Q.

4.10. Discussion of results: freewheeling screw

The basic results of the freewheeling towing tests are illustrated in Fig. 6. Sets of data for three different shaft frictional torque settings are presented. The chart depicts the drag data obtained experimentally for the locked shaft condition also, and for comparison, the corresponding curve predicted using Eq. (1) and $C_D = 1.2$ is included. At the other end of the spectrum, for the hypothetical freewheeling condition with zero braking torque, the curve of predicted drag for $C_D = 0.3$ (Larsson and Eliasson, 1994) is shown also.

Recalling that one of our aims was to evaluate the possible use of the Wageningen B-Screw results to model freewheeling drag characteristics, polynomials were generated to predict K_T and K_Q for the screw being tested, viz.:

$$K_T = 0.1900 - 0.2517J - 0.1904J^2 + 0.07085J^3, \tag{11}$$

$$K_Q = 0.01684 - 0.01777J - 0.01291J^2 + 0.005945J^3. \tag{12}$$

The forward performance curves are depicted in Fig. 7a along with their extrapolations into the zone of negative thrust and negative torque. The section of interest to us is

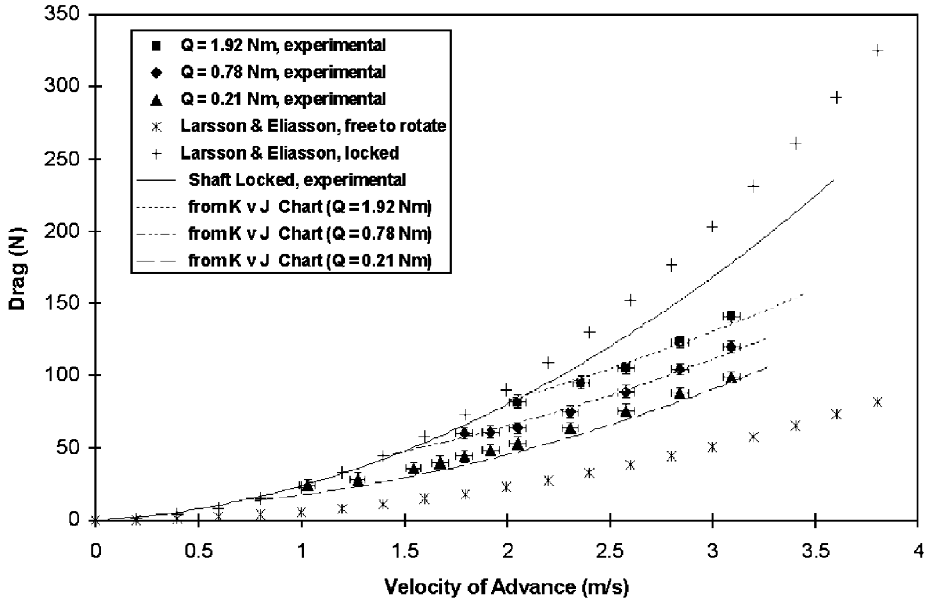

Fig. 6. Freewheeling shaft: results of trials at various shaft torque settings for screw 'A'. Data points and error bars are given for the towing tank experiments on this screw. The curves derived here from K vs. J charts were generated using the K_T and K_Q curves which had been produced using the towing tank data for the same propeller.

shown magnified in Fig. 7b. Also in this figure are the corresponding data points obtained from the towing tank results. The predicted curves in this area are essentially collinear and therefore least-squares regression lines have been fitted through the experimental data for K_T and K_Q.

The experimentally derived linear fits of K_T and K_Q were used to reconstruct curves of drag vs. velocity and these are presented alongside the experimental data points in Fig. 6. It is not surprising that there is good correspondence, the divergence between the reconstructed data and curves through the experimental resistance data being not more than 2% of the drag force.

Fig. 8 contains the curves of drag vs. velocity developed from the coefficients generated by our experimental drag trials, together with those predicted for the equivalent B-Screw. Here the agreement is less good, the differences in drag force being up to 13% for the highest level of shaft torque, and as much as 20% for the lowest torque setting; the proportional difference was generally much less at the lower end of the velocity range. Nevertheless, these data predict drag forces which are in all cases some 100–200% greater than those given by the simple approach described by Larsson and Eliasson.

5. Investigation - locked shaft condition

5.1. Experimental evaluation of drag characteristics

For yachts under sail, this is the set-up most frequently used. Leaving aside the mistaken belief possessed by many yachtsmen that this is the preferred (low drag) configuration, most manufacturers of small marine gearboxes specify that, when their products are fitted in sailing boats, the transmission should be locked by engaging ahead or astern gear when the engine is not in use and the vessel is making way. The reasons for this are generally concerned with durability and wear; for example, some gearbox designs receive adequate lubrication of internal bearings only when the engine is operating.

Tests were conducted using the towing tank and the same experimental arrangements as described for the freewheeling tests detailed above. In addition to the propeller used in the freewheeling tests, two other screws of common patterns were assessed; all three are illustrated in Fig. 5 and their dimensions are detailed in Table 3.

The drag force and velocity data are presented in Fig. 9; these are net of the drag due to the test rig. The figure also incorporates results published by Lurie and Taylor (1995) for three further geometries of fixed-blade propellers and one folding propeller. It can be seen that, despite the differing experimental arrangements employed, namely a towing tank in our case and a water tunnel in the previous work, the results for the fixed-blade screws are of a broadly similar pattern.

We have gone on to reduce the data for all of the propellers to give, in Fig. 9b, C_D values over the speed range of interest. The measured drag forces, along with projected frontal areas, A_P, were reduced to values of C_D for each screw thus:

$$C_D = \frac{T}{0.5 A_P \rho V_A^2}, \tag{13}$$

where, from Gerr (1989), a good approximation of A_P is given by

$$A_P = A_E\left(1.0125 - 0.1\frac{P}{D} - 0.625\left(\frac{P}{D}\right)^2\right). \tag{14}$$

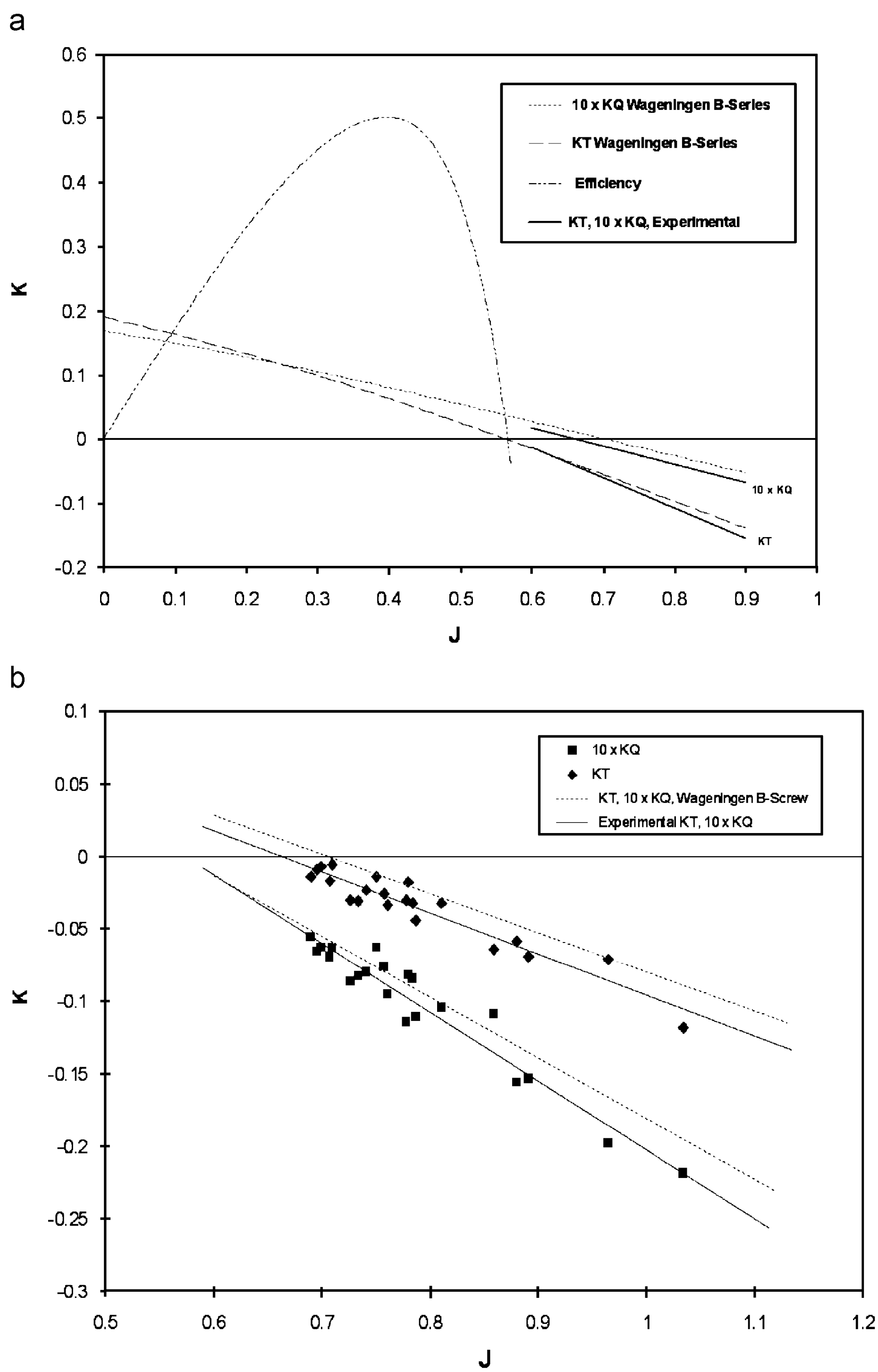

Fig. 7. (a) Freewheeling shaft: predicted and experimental performance chart for screw ‘A’. (b) Freewheeling shaft: predicted and experimental performance chart for screw.

Finally, in order to emphasise the distinct contrast in drag obtained where a folding propeller is in use, we have added results which Lurie and Taylor obtained for a two-blade folding propeller of a pattern which is in widespread use. (Note that the C_D values we have given for the folding propeller are *not* properly the hydrodynamic measure of drag coefficient in that it is the projected frontal area, A_P, of the deployed blades, not that of the folded geometry, which is used as the denominator, whilst the drag forces were those obtained with the folded arrangement; rather we have followed the style of Larsson and Eliasson (1994) who use this as a shorthand method of making practical comparison between configurations. Of course, in the folded configuration, a major element of the drag is due to the bluff body effect of the propeller hub; one should note, therefore, that a change in unfolded blade area would

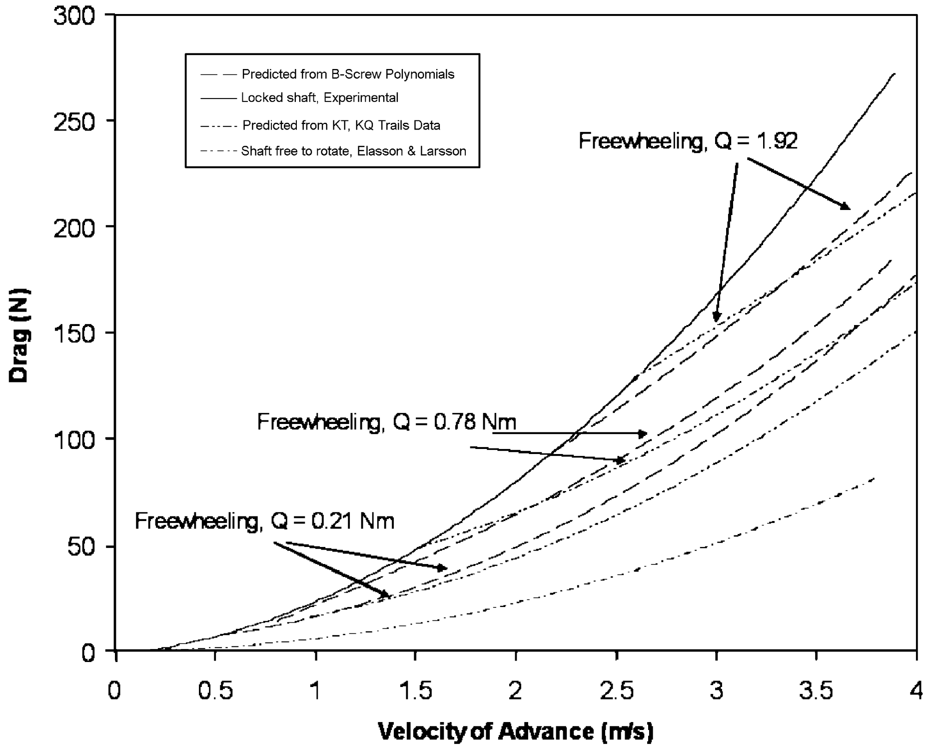

Fig. 8. Freewheeling shaft: characteristics of screw 'A' for three shaft torque conditions. Comparison is here drawn between the curves predicted using B-screw polynomials and those reconstructed from the K_T and K_Q curves derived from towing tank tests on screw 'A'. The upper boundary to the data is set by the curve for the locked condition and the lower boundary is represented by the hypothetical zero-torque case.

Table 3

Propeller	Diameter (m)	Pitch (m)	Expanded area ratio A_E/A_0	Blade section details
Propeller 'A' 12 × 6 in, three-blade	0.305	0.152	0.54	Airfoil from blade root to 0.7 R; remainder of blade ogival. Rake = 6°.
Propeller 'B' 12 × 6 in, three-blade	0.305	0.152	0.52	Airfoil from blade root to 0.5 R; remainder of blade ogival. Negligible rake. Moderately skewed
Propeller 'C' 12 × 8 in, two-blade	0.305	0.203	0.40	Airfoil from blade root to 0.5 R; remainder of blade ogival. Negligible rake
Propeller 'D' 13 × 7 in, three-blade	0.330	0.254	0.44	Combined airfoil/ogival. Negligible rake
Propeller 'E' 13 × 7 in, two-blade	0.330	0.254	0.36	Combined airfoil/ogival. Negligible rake
Propeller 'F', 13 × 7 in, three-blade	0.330	0.254	0.30	Patented airfoil/stepped ogival. Negligible rake

not necessarily be accompanied by a proportional change in hub area, the hub size being determined by other practical requirements such as shaft diameter and torque loadings.)

5.2. Discussion of results: locked shaft

The C_D data for the locked propellers show a surprisingly wide variation in trends for the different patterns of screw. For example, at a velocity of advance of 3.09 m/s (6 knots), $C_D = 0.98 \pm 0.18$, the distribution of C_D values for the six screws is spread almost uniformly across that range, with no clustering around a mean. The overall average for all the data points is 1.08 and is therefore slightly lower than the figure of $C_D = 1.20$ proposed by Larsson and Eliasson. The previously published data for the folding propeller also demonstrate a slightly different average "apparent" coefficient of drag (i.e., the drag being for the folded condition, see above) from that suggested, in this case, being higher, at $C_D = 0.09$ rather than 0.06. The experimentally derived characteristics of the folding propeller have been included in Table 4 for comparison with some other configurations, both locked and freewheeling.

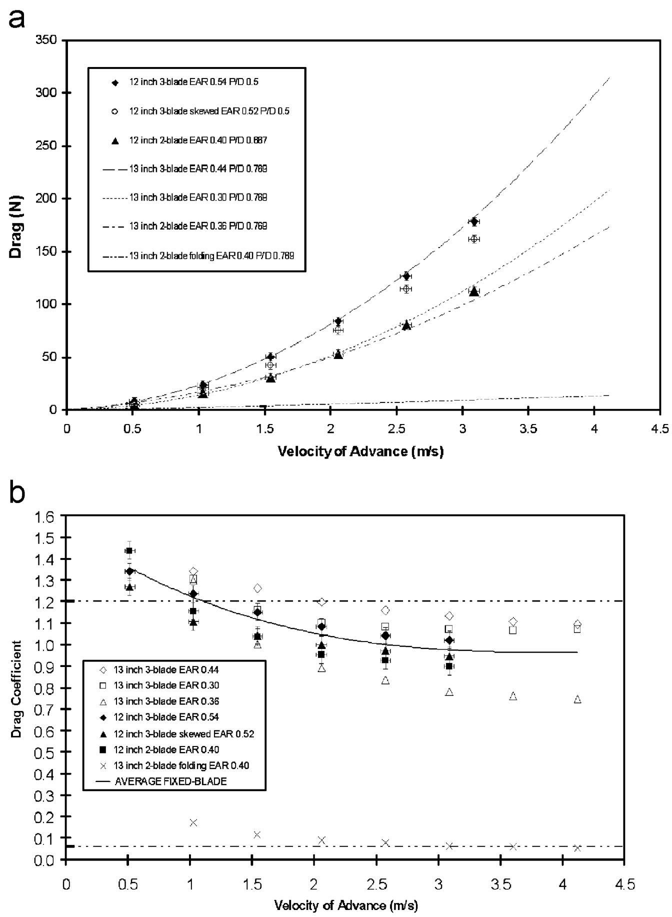

Fig. 9. (a) Locked shaft: summary of experimental evaluations of drag for six fixed-blade screws. The results for a folding propeller illustrate the significant reduction in resistance which can be achieved with such devices. (b) Locked shaft: drag coefficients derived from the data in (a).

6. Case study

In order to demonstrate the significance of these results in the context of the overall resistance of a sailing boat hull, for convenience we may draw on a simple but very approximate relationship between specific resistance of a hull, R/Δ, where Δ is the displacement of the vessel, and the speed-to-length ratio, $V/\sqrt{L}$, where L is the waterline length. The relationship has been presented graphically for a range of displacement-to-length ratios (DLR) by Marchaj (2000). Two cases were considered for our purpose: a moderate displacement boat of DLR $= 200$, typifying a modern cruiser racer; and a heavy displacement yacht with DLR $= 400$, an example of which would be a heavily built ocean-going cruiser. Estimates of the ratio of propeller drag to hull drag at $V = 3.63$ m/s (about 90% of hull speed for the given LWL) are given in Table 4 for each case. For the purposes of the comparison, we have assumed an identical propeller installation in both cases and whilst this is not entirely improbable, it would be unlikely to provide the optimal set-up for mechanical propulsion of the heavy boat, the small propeller lacking somewhat in blade area. (It must also be emphasised the evaluations of

Table 4

Boat type	Displacement to length ratio (DLR)	Displacement Δ (kg)	Waterline length (LWL) (m)	Propeller configuration (1)	Predicted resistance at 3.63 m/s (7 knots) (1)	Propeller configuration (2)	Predicted resistance at 3.63 m/s (7 knots) (2)
Heavy displacement	400	10,800	9.1	0.305 m diameter, 0.152 m pitch, three-blade, EAR = 0.54, Shaft locked	Hull drag 6970 N, Prop drag 239 N	0.305 m diameter 0.152 m pitch, three-blade, EAR = 0.54, Freewheeling, Torque = 0.21 N	Hull drag 6970 N, Prop drag 119 N
Moderate displacement	200	5400	9.1	0.305 m, diameter 0.152 m pitch, three-blade, EAR = 0.54, Shaft locked	Hull drag 3240 N, Prop drag 239 N	0.305 m diameter 0.152 m pitch, three-blade, EAR = 0.54, Freewheeling, Torque = 0.21 N	Hull drag 3240 N, Prop drag 119 N

hull resistance are for illustrative comparisons only and are not intended to be regarded as rigorous assessments of any case in particular.) As can be seen in the table, for the heavier boat, the additional drag due to both the locked propeller (3.4%) and in the freewheeling arrangement (1.7%) is relatively insignificant compared to the respective penalties (14.8% and 7.3%) imparted by the trailing screw in the example of the moderate displacement yacht. Were the heavy boat to be fitted with a larger, perhaps more suitable, screw, then its drag penalty too would, of course, be more harmfully affected. It is worth observing that, in a sailing boat, the driving force is almost directly proportional to the amount of sail area, and therefore the consequence is that those predicted percentages of parasitic drag due to the screw consume the entire driving force produced by an identical proportion of the vessel's sail area.

7. Concluding remarks

The parasitic drag imposed on sailing yachts by a range of propeller set-ups has been investigated. New data generated in towing tank tests has been incorporated with previous independently published findings in order to assess a range of typical two- and three-bladed sailboat propeller configurations in the locked shaft condition. Further experiments were conducted on one of the three-bladed propellers in the freewheeling condition with a range of different frictional torque settings applied to the shaft.

Part of the investigation was directed towards establishing whether the polynomials associated with the Wageningen B-Screw Series could be used to predict the freewheeling performance of sailboat propellers of conventional geometry. This appears to be justifiable to a degree of accuracy which would in most respects be adequate for boat design and screw selection, provided that the blade section is of the common mixed ogival/airfoil pattern, even where the geometry of interest does not mirror precisely the detailed Wageningen standard.

For the freewheeling condition, with a fixed magnitude of braking torque on the shaft, B-Screw polynomials produced significantly better agreement with results of towing-tank experiments than did a previously published approach. The correlation between the polynomial results and experiment was best for the higher torque settings tested; in the worst instance, differences of up to 20% between predicted and experimental drag forces were observed for low torque/high boatspeed conditions.

Aside from B-Screw considerations, it was demonstrated for the three-blade screw tested in freewheeling conditions that K_T and K_Q resistance curves, which were generated purely from experimental data, could be used to predict propeller drag forces with considerable accuracy over the full range of operating conditions.

For the locked shaft condition, a series of new data were generated in towing tank trials and incorporated with other published results of similar work. Six propellers were represented in all, with expanded area ratios from 0.30 to 0.54. The overall average drag coefficient calculated over the entire speed range up to 4.1 m/s was, at $C_D = 1.1$ only marginally less than the single value, $C_D = 1.2$, which had been proposed in earlier work. However, a consistent trend showing the C_D to be significantly dependent on velocity was apparent, and this was especially so at the lower end of the speed range; one may speculate that this may be due to a laminar—turbulent transition (the Reynolds numbers obtained point us towards this) but such a conclusion cannot be supported without further investigation.

This speed-related trend was observed for all six screws tested but, in addition, there were significant differences between the C_D values obtained for each of the propellers at each point in the speed range. One might infer from these observations, taken collectively, that to consider a locked propeller to be a bluff body normal to the flow may be an over-simplification. Nevertheless, where a simplistic prediction of locked-shaft drag is required, an average C_D value of 1.1 could be used but with a caveat that, at the upper and lower ends of the speed range tested, C_D values diverging by as much as 30% from this have been observed, depending on the particular propeller geometry being considered.

The experimental results confirm that a locked propeller produces greater drag than does a freewheeling screw (up to 100% more drag was observed, this being at higher speeds). Furthermore, for the freewheeling case, the magnitude of the hydrodynamic resistance is significantly affected by the amount of frictional torque on the shaft, low torque being accompanied by low drag.

Finally, a simple model of sailboat hull resistance has been used to illustrate the likely scale of the drag penalty due to various arrangements of trailing propeller. This shows that, especially for the case of craft having moderate or low DLR combined with powerful mechanical installations, the impact on sailing performance of a trailing propeller is very significant indeed. By combining the present findings with other more detailed techniques which exist for modelling hull drag, the influence of propeller drag on sailing performance should be substantially predictable.

References

Benini, E., 2003. Multiobjective design optimization of B-screw series propellers using evolutionary algorithms. Marine Technology 40, 229–238.

Gerr, D., 1989. Propeller Handbook. International Marine, Camden ME, US.

Henderson, R., 1983. The Racing Cruiser. International Marine, Camden ME, US.

Johnson, P., 1997. Yacht Rating. Bucksea Guides, Lymington, UK.

Larsson, L., Eliasson, R., 1994. Principles of Yacht Design. Adlard Coles Nautical, London, UK.

Lurie, B., Taylor, T., 1995. Comparison of ten sailboat propellers. Marine Technology 32, 209–215.

Marchaj, C.A., 2000. Aero-Hydrodynamics of Sailing, third ed. Adlard Coles Nautical, London, UK.
Oosterveld, M.W.C., van Oossanen, P., 1975. Further computer-analyzed data of the Wageningen B-screw series. International Shipbuilding Progress 22, 251–262.
Skene, N.L., 1938. Elements of Yacht Design, sixth ed. Sheridan House, Dobbs Ferry NY (US reprinted 2001).
van Lammeren, W.P.A., van Manen, J.D., Oosterveld, M.W.C., 1969. The Wageningen B-screw series. Transactions of the SNAME 77, 269–317.
van Manen, J.D., van Oossanen, P., 1988. Propulsion. In: Lewis, E.V. (Ed.), Principles of Naval Architecture, Vol. 2. Society of Naval Architects and Marine Engineers, Jersey City, NJ, US.
Warren, N., 1972. Prop drag. In: *Practical Boat Owner*, vol. 72, pp. 114–115.